PAPER

The electrochemistry of neptunium in tri-*n*-butyl phosphate

Joshua R. Dunbar [ID] [a] and Mark P. Jensen [ID] *[a,b]

Neptunium's electrochemical behavior was studied in solutions of undiluted, acid-equilibrated tri-*n*-butyl phosphate (TBP) as well as in TBP solutions diluted by dodecane. Careful experimental choices and electromagnetic noise suppression allowed voltammetry in the low-conductivity 30 vol% TBP/*n*-dodecane solvent, bypassing the approximation of using undiluted TBP for this widely used solvent composition. In undiluted TBP, the Np(VI/V) couple is quasireversible and has a half-wave potential of 0.722 ± 0.012 V *vs.* Ag/AgCl. Diffusion coefficients for the Np(VI) and Np(V) species were found to be $(4.3 \pm 0.8) \times 10^{-7}$ cm^2 s^{-1} and $(3.5 \pm 0.6) \times 10^{-7}$ cm^2 s^{-1}, respectively. The Np(IV/III) couple is irreversible in TBP indicating that Np(III) is unstable; however, like the Np(VI/V) couple, it shows stabilization of the more-oxidized state by TBP complexation. Spectrophotometry showed that Np(V) is unstable in undiluted TBP–HNO$_3$, oxidizing to Np(VI) over time. Switching macroelectrodes for ultramicroelectrodes enables measurement of neptunium redox couples in TBP diluted with dodecane, and increased dilution shifts the Np(VI/V) couple to more negative potentials. Voltammetry in even 30 vol% TBP was possible with a minor amount of supporting electrolyte. The presence of di-*n*-butyl phosphoric acid (HDBP), a common TBP radiolysis product, stabilizes Np(VI) relative to Np(V), with exchange of one HDBP upon reduction of Np(VI).

Introduction

In light of the renewed global interest in nuclear energy, advanced reprocessing schemes are being considered to close the nuclear fuel cycle. For nuclear fuel reprocessing to be a viable option, it is essential to enhance the efficiency of actinide separations by increasing product purity and reducing the number of separation stages required to achieve that purity.[1]

A variety of reprocessing schemes are being touted as advances over the historical PUREX separation process,[2] such as the CoDCon,[3] the European GANEX processes,[4] and others.[5] In these schemes, redox control takes a central role in routing actinides through the process. The PUREX process uses an extractant solution of 30 vol% tri-*n*-butyl phosphate (TBP) in kerosene to extract uranium and plutonium from nitric acid solutions of used nuclear fuel. Redox control is important because only tetra- and hexavalent actinides are extracted by TBP under these conditions, but key actinide elements like neptunium and plutonium also can exist as unextractable Np(V) or Pu(III) during these separations.

Despite the importance of organic-phase redox reactions for efficient separations, they have received far less attention than their aqueous counterparts. Some studies have investigated the kinetics of chemical reductants for the Np(VI/V) reduction in the organic phase,[6,7] but detailed electrochemical insight has been lacking. This is in large part due to the nature of TBP as a solvent, as TBP diluted in kerosene, the solvent used for nuclear reprocessing, will have a very low conductivity (20 μS cm^{-1}) on its own[8] and the strongly nonpolar nature of the diluent limits the utility of supporting electrolytes. In undiluted TBP, Mokhtari and Picart obtained reduction potentials for the Pu(IV/III) and Am(VI/V) couples with a tetrabutylammonium triflate supporting electrolyte and an ultramicroelectrode.[9] Bahri *et al.* have measured both the Pu(IV/III) and Pu(VI/V) couples in neat (100%) TBP, and they determined that the conductivity due to coextraction of acid and water by TBP was enough to support conventional voltammetry for the Ce(IV/III) couple in solutions containing as little as 65 vol% TBP in dodecane.[8,10] (All percentages referring to TBP concentration in this paper are volume percent.) Voltammetry of neptunium complexed to TBP has also been performed in ionic liquid media.[11] However, neptunium has not been the subject of electrochemical analysis in reprocessing-relevant molecular organic phases.

Redox control of neptunium is a particularly important and challenging aspect of nuclear fuel reprocessing, as both Np(IV) and Np(VI) are extracted well by TBP, while Np(V) is nearly unex-

[a]Chemistry Department, Colorado School of Mines, Golden, CO 80401, USA.
E-mail: mjensen@mines.edu
[b]Nuclear Science and Engineering Program, Colorado School of Mines, Golden, CO 80401, USA

tractable.[12] Multiple factors influence neptunium oxidation state speciation in industrial-scale processes, including oxidation by nitric acid[13] and radiolysis-induced redox transformations.[14] Radiolysis of the organic phase also modifies actinide redox behavior, due to the production of di-*n*-butyl phosphoric acid (HDBP) from both radiolytic and acid-catalyzed degradation of TBP.[15,16] Electrochemical investigations of the Ce(IV/III) couple (an actinide surrogate) have shown that HDBP stabilizes Ce(IV) in TBP phases.[8,17] Solvent extraction studies also have suggested that HDBP stabilizes Np(VI) in TBP organic-phases in addition to increasing its extraction,[18] but HDBP–actinide interactions have not yet been probed by voltammetry. In current industrial reprocessing plants, the sum of these effects is that approximately 75% of neptunium is routed with uranium and plutonium to the organic phase in the first extraction step,[19] illustrating the need for insight into neptunium redox in order to achieve improved separations.

In their study of the Ce(IV/III) couple in TBP, Bahri *et al.* have shown that the Ce reduction potential shifts to lower values changing from undiluted, acid-equilibrated TBP to 65% TBP.[8] Thus, in investigating the organic-phase electrochemistry of neptunium, it is key to closely approximate the industrial solvent composition – otherwise, results may have less relevance to real-world systems. To this effect, we have extended the work of previous authors[8–10] to achieve voltammetric analysis in 30% TBP through innovations such as miniaturization of the working electrode, use of a coated wire quasireference electrode,[20] and prudent choice of supporting electrolyte.

In this work we present the voltammetry of neptunium in neat and diluted TBP systems, with attention paid to re-creating process-relevant solvent compositions. The Np(VI/V) and Np(IV/III) couples were investigated first in undiluted TBP, and results demonstrate that both Np(VI) and Np(IV) are stabilized through complexation by TBP. Spectrophotometric results show that the Np(V) state is unstable in undiluted, acid-equilibrated TBP and will oxidize to Np(VI). Investigation of the Np(VI/V) couple in TBP/dodecane mixtures with as little as 30% TBP demonstrated that decreasing the TBP concentration shifts the position of the Np(VI/V) couple to lower potentials. In TBP/*n*-dodecane solutions, the presence of HDBP stabilizes Np(VI) against reduction, illuminating a mechanism by which radiolytic HDBP interferes with reprocessing separations.

Experimental methods

Caution! [237]Np with a half-life of 2.14 million years is a radiotoxic, alpha emitting heavy metal, and therefore care must be taken while using it. Operations involving the handling of radioactive solutions containing [237]Np must be done with proper engineering controls such as radiological fume hoods or gloveboxes. Protective gloves, glasses, and other appropriate controls must be in place during experiments involving these radioactive materials.

Reagents

Tri-*n*-butyl phosphate (99+%, Acros Organics) was purified prior to use using the method of Yoshida.[21] This purification involved subsequent triplicate washes with HNO$_3$ (0.2 M), NaOH (0.2 M), and deionized water, followed by vacuum distillation. Di-*n*-butyl phosphoric acid (97%, Acros Organics), *n*-dodecane (99%, Thermo), tetra-*n*-butylammonium triflate (99%, Alfa), and tetra-*n*-butylammonium tetrafluoroborate (99%, Sigma) were used as received. Solutions of nitric acid were prepared by dilution of concentrated acid (68% ACS grade) with 18.2 MΩ cm deionized water. Prior to use, TBP solutions were equilibrated with the desired concentration of nitric acid by triplicate contacts of equal volumes of the TBP solution and aqueous acid.

Neptunium solutions

A [237]Np stock solution was made by dissolution of solid NpO$_2$ in hot 8 M HNO$_3$ followed by purification on a Bio-Rad AG 1-X4 anion exchange column, where plutonium contamination was removed by washing the column with 0.1 M semicarbazide and 0.01 M ferrous sulfamate in 4.5 M HNO$_3$.[22] Isotopic purity was confirmed *via* alpha spectrometry. Aliquots of the neptunium stock solution were diluted into the appropriate concentration of nitric acid and were adjusted to Np(IV) or Np(VI) by bulk electrolysis before extraction into TBP. Bulk electrolysis was performed using a three-compartment fritted "W" cell with no dead volume[23] (Adams & Chittenden Scientific Glass, P4 frits, SI Fig. S1) using Pt working and counter electrodes and a Ag/AgCl reference electrode. The working electrode potential was set to +1.3 V *vs.* Ag/AgCl to prepare Np(VI) and to −0.2 V for Np(IV) preparation.[24] Oxidation state purity was confirmed by optical spectroscopy using a Cary 5E UV-vis-NIR spectrophotometer to monitor the Np(IV) absorptions at 700 and 960 nm as well as the Np(V) absorption at 980 nm and the Np(VI) peak at 1225 nm. Neptunium was loaded into organic phases through a single contact of a nitric acid solution containing neptunium in the appropriate oxidation state with pre-equilibrated TBP.

Electrochemical experiments

A Metrohm Autolab PGSTAT302N potentiostat was used for all experiments. For investigations in undiluted TBP, a 1 mm diameter glassy carbon electrode (GCE) and Ag/AgCl (3 M NaCl) reference electrode (RE) were purchased from Bioanalytical Systems, Inc. In experiments using TBP diluted with *n*-dodecane, a 10 μm Pt ultramicroelectrode (UME) from Bioanalytical Systems, Inc. was used as the working electrode along with a freshly prepared platinum–polypyrrole (Pt/PPy) quasireference electrode (QRE). The synthesis and characterization of Pt/PPy QREs has been reported previously.[8,20] Briefly, this consisted of cycling a 0.5 mm Pt wire 50 times at 100 mV s^{-1} between −0.6 V and +1.175 V *vs.* Ag/AgCl in a solution of 0.1 M tetra-*n*-butylammonium tetrafluoroborate and 10 mM pyrrole in acetonitrile. On the last cycle the potential was held at +0.7 V for 30 seconds to partially oxidize and dope the film with anions, followed by rinsing the electrode with water. The potential of the Pt/PPy electrode was measured against an

Ag/AgCl electrode in a 50% TBP solution (pre-equilibrated with 4 M HNO_3) before and after experiments. The GCE and UME were polished with 0.05 μm alumina prior to use, and all TBP electrochemistry was performed under argon, sparging the solution for 15 minutes beforehand. Ultramicroelectrode current traces were smoothed in the NOVA 2.1 potentiostat control software using a Savitzky–Golay polynomial filter (SI Fig. S2 shows the extent of smoothing). All electrochemical potentials are given referenced to the Ag/AgCl electrode unless otherwise noted. Solution conductivities were measured with a VWR glass probe conductivity meter tested against KCl solutions of known conductance, which provided measured values within 2% of expectation. Uncertainties on measured quantities are given at the 95% confidence interval.

Organic-phase bulk electrolysis

Preparation of Np–TBP solutions with varying Np(VI) : Np(V) ratios was performed similarly to aqueous bulk electrolysis. Neat TBP equilibrated with 1 M HNO_3 and containing 0.1 M tetra-*n*-butylammonium triflate (TBA OTf) was used as the solvent, and Pt was used for working electrode (WE) and counter electrode (CE) with an Ag/AgCl RE. Prior to electrolysis, a cyclic voltammogram was collected on the Np–TBP solution directly in the center compartment of the "W" cell using a GCE. Spectrophotometric measurements were collected in a 1.00 cm optical glass cuvette on aliquots of solution removed from the WE (center) compartment of the "W" cell.

Results

Undiluted TBP

Because of the relatively good conductivity of neat TBP equilibrated with 4 M HNO_3 (calculated $[HNO_3]_{org}$ = 2.37 M and $[H_2O]_{org}$ = 1.91 M;[25] conductivity listed in SI Table S1), the voltammetry of the Np(VI/V) couple in this medium is tractable. Hexavalent neptunium in TBP exists as $NpO_2(NO_3)_2 \cdot 2TBP$.[26] A series of cyclic voltammograms of the Np(VI/V) couple at different scan rates in undiluted, acid-equilibrated TBP are shown in Fig. 1a, where clean oxidation and reduction peaks for this redox event are visible.

The half-wave potential $E_{1/2}$, which is a reasonable estimate of the formal potential, is 0.722 ± 0.012 V *vs.* Ag/AgCl for the Np(VI/V) couple in this medium. This substantial negative shift from the Np(VI) reduction potential in aqueous 3 M HNO_3 (measured as 0.886 V *vs.* Ag/AgCl by cyclic voltammetry[27]) reveals that Np(VI) is stabilized through TBP complexation. After subtraction of background CVs, the peak currents for each CV were calculated and found to be linear with respect to the square root of scan rate (Fig. 1b). By the theory of the Randles–Sevcik equation, this indicates that the Np(VI/V) couple is operating in the diffusion-controlled regime at the electrode surface. Thus, diffusion coefficients for each species may be calculated from the equation, which at 25 °C is

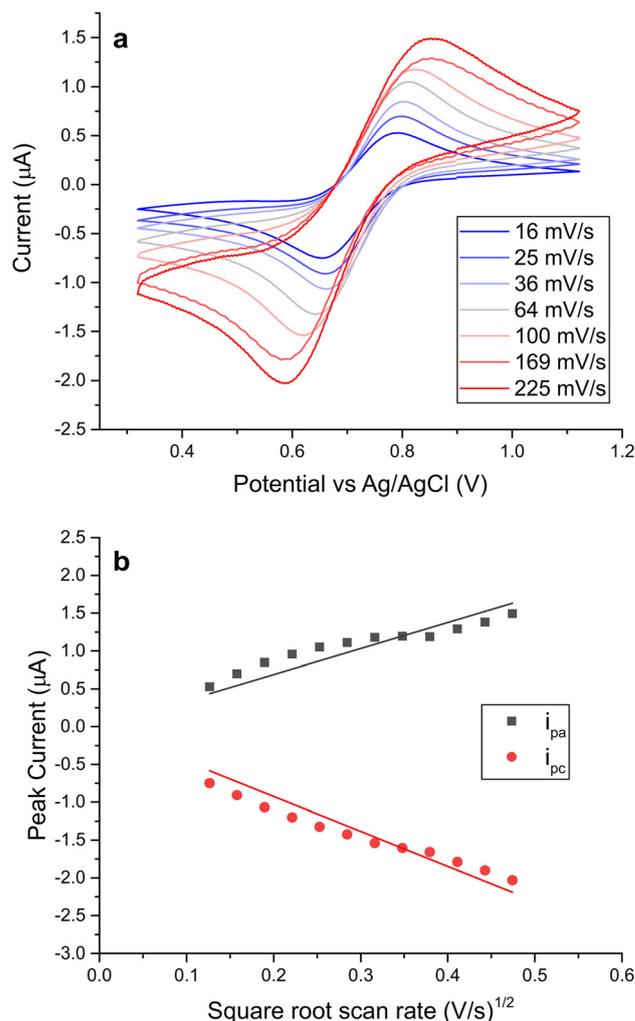$$i_p = 2.69 \times 10^5 n^{3/2} AC\sqrt{Dv} \qquad (1)$$

Fig. 1 (a) Background-subtracted cyclic voltammograms of varying scan rate at the Np(VI/V) couple. The solution was prepared by extracting Np(VI) from 4 M HNO_3 into pre-equilibrated neat TBP. Working electrode: glassy carbon; counter electrode: Pt coil; reference electrode: Ag/AgCl; [Np] = 3.68 mM; scan rate: 16–225 mV s^{-1}. (b) Peak currents from cyclic voltammograms of various scan rates plotted against the square root of scan rate. The least-squares fit with zero intercept is indicated by the solid lines.

where i_p is the CV peak current, n is the number of electrons transferred, A is the electrode area (cm^2), C is the electroactive species concentration (mol cm^{-3}), D is the diffusion coefficient (cm^2 s^{-1}), and v is the scan rate in V s^{-1}. The resulting calculation indicates that for Np(VI), the diffusion coefficient is (4.3 ± 0.8) × 10^{-7} cm^2 s^{-1} and for Np(V), it is (3.5 ± 0.6) × 10^{-7} cm^2 s^{-1}. While the organic-phase neptunyl speciation differs from that in aqueous media, Chatterjee *et al.* also observed a smaller diffusion coefficient for Np(V) than Np(VI) in aqueous nitric acid.[28]

Because of the wide solvent window enabled by using inert glassy carbon (GC) working electrodes in the TBP–HNO_3 medium, wider scan voltammograms were collected for a solution with Np(VI) as the bulk oxidation state. A representative

scan in neat TBP equilibrated with 4 M HNO$_3$ is shown in Fig. 2 (background scan over same region shown in SI Fig. S3).

In Fig. 2, the Np(VI/V) couple is visible in the positive potential region, and new redox events have appeared in the negative potential region with clearly irreversible kinetics. The cathodic reduction peak, E_{pc}, appears at −0.494 V vs. Ag/AgCl, and the anodic oxidation peak, E_{pa}, has a potential of −0.189 V. The peaks for this low-potential activity have dramatically asymmetric peak currents, and the fast current rise for the reductive sweep suggests that the observed reduction is not a simple two-electron event. In fact, by considering that the Np(V) concentration at the electrode surface is equal to the bulk neptunium concentration when a >1 V reduction overpotential is applied,[29] the Randles–Sevcik equation (eqn (1)) may be used to relate the peak current of the one-electron Np(VI) reduction at 0.583 V with that of the event at −0.494 V. This relation yields the number of electrons transferred in the new reduction event, n = 2.2 ± 0.2. While the large reduction current at low potentials provides information about the electron transfer stoichiometry of this event, the diminutive size of the corresponding oxidation event sheds light on the kinetic stability of the species involved. Even after background subtraction, only a small oxidation current is observed, and this feature is only observed in the first CV sweep – subsequent sweeps have no oxidation peak. Thus, the species involved in the oxidation is kinetically unstable.

Because of its higher resolving power and ability to minimize background currents, differential pulse voltammetry (DPV) was chosen to further investigate neptunium behavior over a wide potential range. Fig. 3 depicts an example DPV (pulse height = 25 mV) in pre-equilibrated neat TBP over the same potential range as Fig. 2 (SI Fig. S4 shows a DPV over
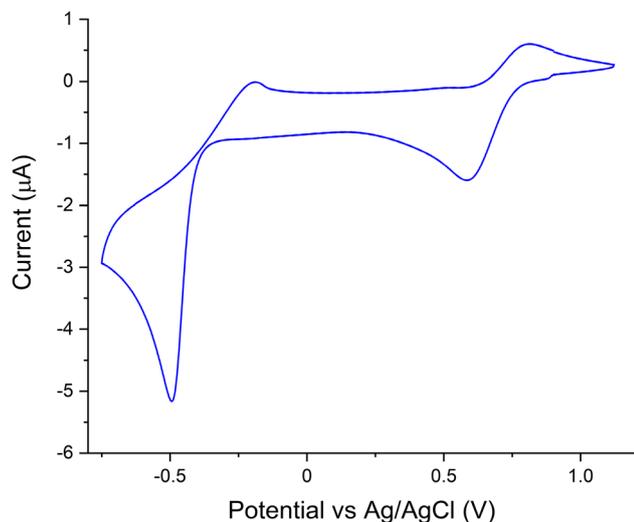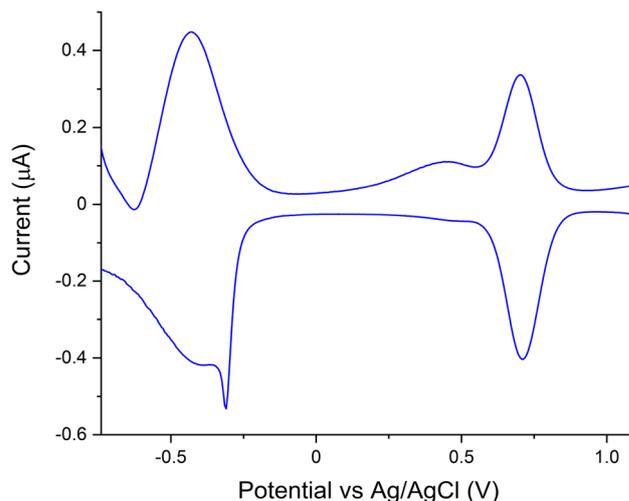

Fig. 3 Wide-window differential pulse voltammogram showing multiple oxidation and reduction events. The solution was prepared by extracting Np(VI) from 4 M HNO$_3$ into pre-equilibrated neat TBP. Working electrode: glassy carbon; counter electrode: Pt coil; reference electrode: Ag/AgCl; [Np] = 3.68 mM.

only the Np(VI/V) region). Immediately visible are the peaks for the Np(VI/V) couple at an average value of 0.709 V. An additional small/broad redox event is observed at approximately 0.45 V; this is a background event and is not neptunium-related. Further DPV scans of TBP–HNO$_3$ to which low concentrations of HNO$_2$ had been added demonstrate that this redox event is caused by small amounts of HNO$_2$ in the TBP–HNO$_3$ solvent (see SI Fig. S5 and accompanying discussion).

The broader peaks at low potentials in both scan directions of the DPV have an average potential of −0.409 V vs. Ag/AgCl, while the sharp event in the negative sweep appears at −0.310 V. This sharp peak was repeatedly observed across multiple scans on different days. Comparing the difference in peak potentials between negative and positive sweeps for the Np(VI/V) couple and the low-potential couple, the Np(VI/V) couple has a 7 mV split, while the low-potential couple shows a more significant shift with a 38 mV split.

The results of the large-window scan of the bulk-Np(VI)–TBP solution prompted investigation of the Np(IV/III) couple in the same medium; however, attempts at obtaining a useable CV were unsuccessful. Currents indicating reduction were observed, but the lack of corresponding oxidation current even at fast scan rates indicated irreversible behavior due to Np(III) being unstable toward oxidation. A representative DPV for the Np(IV)–TBP solution is shown in SI Fig. S6, where the positive and negative sweep peak potentials occur at −0.51 V and −0.45 V, respectively. This substantial negative shift when compared with the aqueous Np(IV) reduction potential (−0.10 V in 1.79 M HNO$_3$)[28] indicates substantial stabilization of the Np(IV) state.

Similar to Fig. 2 and 3, wide-range CV and DPV scans were attempted over the range −0.75 V to +1.1 V in the Np(IV)-containing neat TBP solution. However, no additional redox events were observed, in contrast to results obtained when

Fig. 2 Background-subtracted cyclic voltammogram showing multiple oxidation and reduction events. The solution was prepared by extracting Np(VI) from 4 M HNO$_3$ into pre-equilibrated neat TBP. Working electrode: glassy carbon; counter electrode: Pt coil; reference electrode: Ag/AgCl; [Np] = 3.68 mM; scan rate: 100 mV s^{-1}.

scanning a Np(vi)-containing solution. SI Fig. S7 depicts CVs taken over the Np(vi/v) couple region of potentials and shows a lack of redox activity in the solution with Np(iv) as the bulk oxidation state. Together with the results of Fig. 2 and 3, this lack of evidence for a Np(iv/v) couple in the potential window scanned demonstrates the kinetic difference between breaking the oxo bonds of Np(v) and re-forming them.

As a final method of characterizing neptunium redox activity in undiluted TBP, bulk electrolysis coupled with spectrophotometry was employed to interrogate the neptunium couple at ~0.7 V *vs.* Ag/AgCl. A Np(vi)–laden undiluted TBP–HNO_3 phase (1 M HNO_3 pre-equilibration; calculated $[HNO_3]_{org}$ = 0.82 M and $[H_2O]_{org}$ = 3.21 M)[25] was subjected to bulk electrolysis, with vis-NIR spectra taken of aliquots of solution removed from the electrolysis cell as the electrolysis progressed. Fig. 4a shows the evolution of the spectra as a function of overpotential *vs.* the $E_{1/2}$ of the redox reaction (measured *via* CV; see SI Fig. S8). In TBP, the Np(vi) absorption at 569 nm is sharper and more highly absorbing than the peak near 1200 nm, so it is used for further analysis.[30] Overall, the Np(vi) concentration decreases as less positive overpotentials are applied, showing that reduction is occurring (Fig. 4b). (See the Discussion section for calculation of molar absorptivities used to obtain concentrations.) The Np(v) absorption region shown in Fig. 4a has the characteristic sharp absorption at 977 nm, in addition to a small peak at 1086 nm also corresponding to Np(v) (see SI Fig. S9). For decreases in overpotential to approximately 0 mV, the Np(v) concentration increases (Fig. 4b). This clearly identified the redox activity at ~0.7 V as the one-electron Np(vi/v) couple.

After a near-zero overpotential was applied to the Np(vi/v) solution, little further decrease in Np(vi) concentration was observed, and the concentration of Np(v) decreased to some extent. Spectra were also taken 30 minutes apart on the solution after application of a −52 mV overpotential, and while the Np(v) concentration immediately after bulk electrolysis was 0.15 mM, the later scan revealed a six-fold decrease to only 0.03 mM (SI Fig. S9). Thus, as observed previously, Np(v) is unstable in the neat TBP–HNO_3 medium.[30] Throughout the entirety of the experiment, no absorptions for Np(iv) at 709 nm or for a Np(v)–Np(iv) cation–cation interaction at 1004 nm were observed.[30,31]

Diluted TBP

With an understanding of neptunium voltammetry in neat TBP–HNO_3 systems, attention was turned to systems containing TBP diluted with dodecane, which are representative of industrial separations. Several important experimental modifications were made to overcome difficulties associated with measurements in low-conductivity, low-dielectric solutions (see SI Table S1 for conductivity of TBP as a function of dilution). First, the working electrode was miniaturized from a 1 mm diameter GC electrode to a 10 μm diameter platinum ultramicroelectrode (UME). The electrochemical cell was also moved into two nested Faraday cages to suppress electrical noise. Finally, the Ag/AgCl reference electrode was switched for
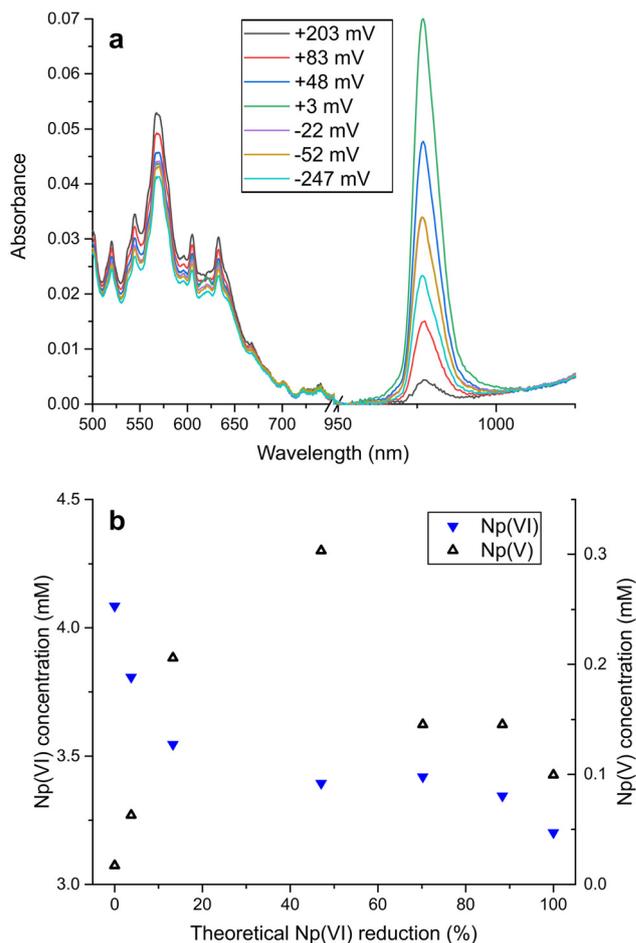

Fig. 4 Spectra of a pre-equilibrated undiluted TBP initially containing Np(vi) extracted from 1 M HNO_3 after organic-phase bulk electrolysis at various overpotentials *versus* the $E_{1/2}$ of the Np(vi/v) couple. Working and counter electrodes: Pt coil; reference electrode: Ag/AgCl; [Np] = 3.78 mM; [TBA OTf] = 0.1 M. (a) Spectra showing Np(vi) and Np(v) absorptions; (b) concentrations for Np(vi) and Np(v) (*via* the 569 nm and 977 nm peaks, respectively) plotted *vs.* theoretical amount of Np(vi) reduced. Estimates of errors in the concentrations are ±8% for Np(vi) and ±15% for Np(v).

a platinum/polypyrrole (Pt/PPy) quasireference electrode (QRE) to minimize liquid–liquid junction potentials.[8] The reported potentials have been converted to the Ag/AgCl reference for continuity.

While CV scans on the UME were obtained for the Np(vi/v) couple in neat TBP and TBP/dodecane solutions, they were generally more qualitative in nature than UME DPV scans (pulse height = 50 mV), which still have a clear peak potential. Differential-pulse voltammetry removes the capacitive charging current component of the voltammetric response, which is particularly important in the low-dielectric solutions of diluted TBP. Additionally, while the positive DPV sweep resulted in repeatable peaks, the negative sweep generally did not produce clear peaks. Similar behavior was observed in the UME CV of neptunium in neat TBP, where the positive sweep generates

identical current traces across multiple scans, but the negative sweep does not (SI Fig. S10).

Fig. 5a renders the change in DPV response for the Np(VI/V) couple as 100% TBP pre-equilibrated with 4 M HNO₃ is serially diluted with dodecane. Overall, the peak potential for the Np(VI/V) redox shifts to lower potentials as the TBP concentration decreases, indicating a stabilization of Np(VI). The peak potential for 100% TBP of 0.701 V is in good agreement with that obtained by DPV with a macro GC electrode (Ag/AgCl reference), which was 0.709 V. The peak current in Fig. 5a also decreases (in keeping with the reduction in neptunium concentration). At the 40% TBP level, the poor electrical characteristics of the solvent arising from reduced organic-phase water and nitric acid concentrations (SI Table S1) begin to severely distort the DPV response, and at 30% TBP without added elec-

trolyte, no useable peak is obtained. With added electrolyte, adequate conductivity is restored and the 30% TBP solution yields good DPV results (*vide infra*). Plotting the peak potentials of Fig. 5a against the logarithm of the molar TBP concentration for Nernst analysis yields a straight line with a slope of 101 ± 26 mV. This slope is intermediate to a slope of either 59 mV or 118 mV, which would be expected for addition of one or two ligands upon a one-electron reduction, respectively.

Without supporting electrolyte, electrochemical analysis of neptunium in 30% TBP did not yield useable results. However, the addition of 20 mM supporting electrolyte – in this case, tetrabutylammonium triflate – enabled satisfactory DPV and CV scans (Fig. 6). This electrolyte concentration causes an increase in conductivity from 4.54 μS cm⁻¹ to 16.17 μS cm⁻¹. For comparison of the electrochemical responses see SI Fig. S11 and S12, which show no-electrolyte DPV and CV scans, respectively. Whereas without electrolyte the DPV current did not decrease as lower potentials were scanned, Fig. 6 shows well-resolved peaks for both sweep directions (0.606 V for positive and 0.451 V for negative sweep directions). Repeated scans after the initial one demonstrated significant variability in the position of the peak on the negative sweep (for example, moving to +20 mV *vs.* the positive sweep peak). Similar behavior has been observed in the reduction-sweep current for CVs of plutonium in neat TBP–HNO₃, where events due to non-diffusion-controlled adsorption-based processes were reported.[10] The presence of electrolyte also improved the CV response at the UME in 30% TBP; whereas in 100% TBP the oxidation and reduction sweeps of a 6 mV s⁻¹ CV were separated by 135 mV, for electrolyte-containing 30% TBP, the separation was only 30 mV, much closer to the expectation of identical scans in either sweep direction.
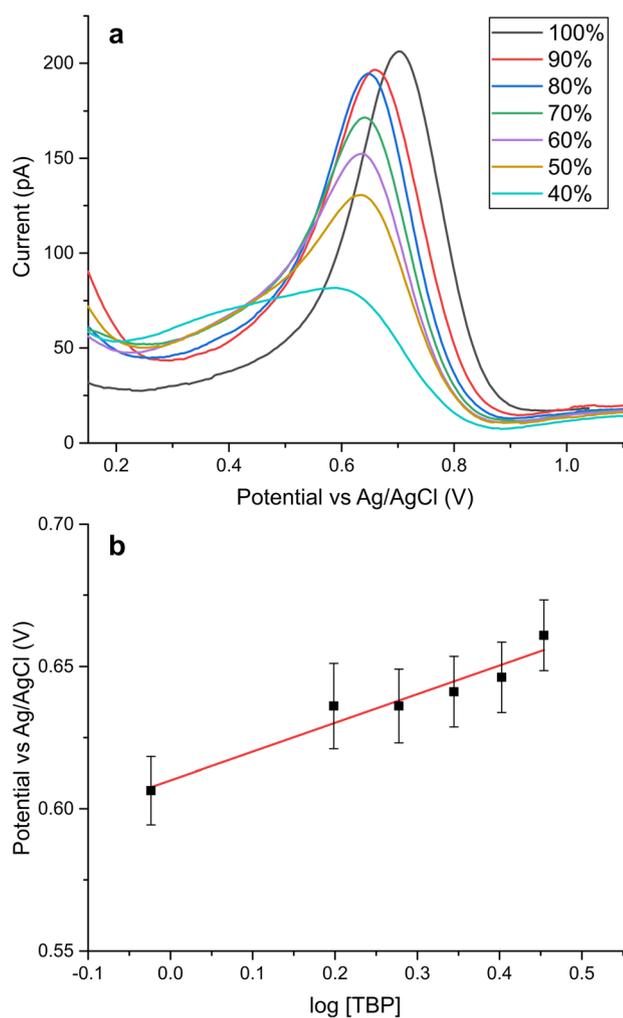

Fig. 5 (a) Differential pulse voltammograms demonstrating the effect of TBP dilution with dodecane on the position of the Np(VI/V) couple. Working electrode: 10 μm Pt ultramicroelectrode; counter electrode: Pt coil; reference electrode: Pt/PPy; initial [Np] = 3.8 mM. (b) Dependence of the DPV peak potential for the Np(VI/V) couple on the logarithm of TBP concentration. The line is the least-squares fit line and is described by $E_p = (0.101 \pm 0.026)\log[\text{TBP}] + (0.610 \pm 0.008)$ with $R^2 = 0.936$.
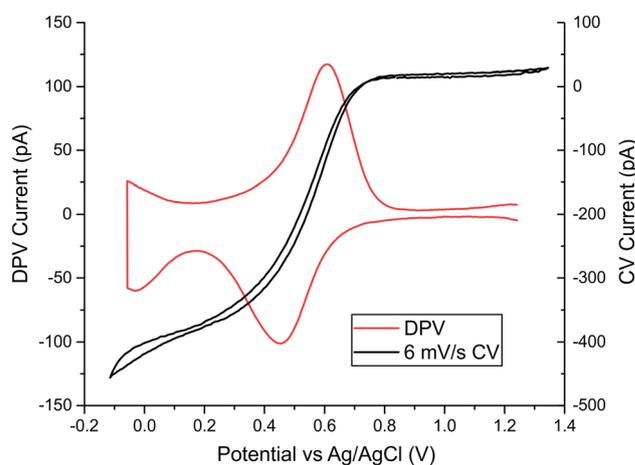
Fig. 6 Cyclic voltammogram and differential pulse voltammogram showing the position of the Np(VI/V) couple in 30% TBP equilibrated with 4 M HNO₃ and containing TBA OTf electrolyte. Working electrode: 10 μm Pt ultramicroelectrode; counter electrode: Pt coil; reference electrode: Pt/PPy; [Np] = 1.1 mM; [TBA OTf] = 20 mM; CV scan rate: 6 mV s⁻¹.

Besides an understanding of how the Np(vi/v) reduction potential changes between the more accessible experimental conditions of neat TBP and the industrially relevant 30% TBP composition, it is also valuable to learn the impact of TBP radiolysis on neptunium oxidation state stability in dilute TBP systems. To obtain better conductivity and electrode response without the use of electrolyte, it was decided to study the effect of HDBP in 50% TBP equilibrated with 4 M HNO$_3$. Fig. 7a shows the evolution of the DPV response as a function of HDBP concentration. The chosen range of HDBP concentration corresponds to an estimated gamma radiolysis dose range of 0 to 315 kGy.[32]

Increased concentrations of HDBP in 50% TBP yield a decrease in the DPV peak potential from 0.691 V vs. Ag/AgCl

without HDBP to 0.545 V with 32 mM HDBP. Additionally, while the neptunium concentration stays virtually constant through the experiment, the peak current decreases, accompanied by widening of the peak. The broader, weaker peaks at higher HDBP concentrations are a likely indicator of decreasing reversibility caused by HDBP. When the DPV peak potentials are plotted against the logarithm of HDBP concentration, a linear trend is obtained with a slope of 54 ± 15 mV per decade (Fig. 7b). This Nernst analysis slope is within error of the 59 mV per decade slope that would be expected for a one-electron redox event involving the transfer of one ligand at 25 °C (see derivation in SI). Because of the use of an ultramicroelectrode and no electrolyte, this experiment in 50% TBP should follow the effect of radiolytically-generated HDBP in a real 30% TBP PUREX-type extraction circuit.
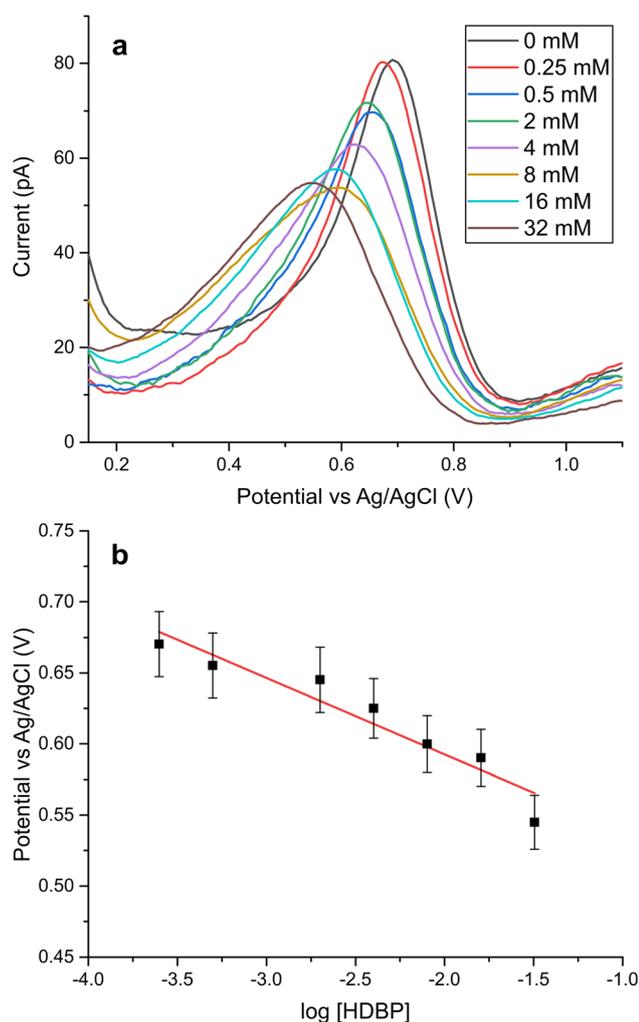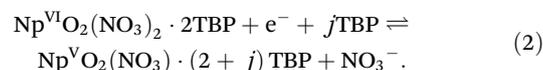
Discussion

Hexavalent neptunium is known to be extracted by TBP as the NpO$_2$(NO$_3$)$_2$·2TBP complex.[26] Generally, interconversion between Np(vi) and Np(v) is reported to be quasireversible (in, for example, aqueous nitric acid).[28] The likely equation for Np(vi) reduction in TBP may be represented as follows:

$$Np^{VI}O_2(NO_3)_2 \cdot 2TBP + e^- + jTBP \rightleftharpoons$$
$$Np^{V}O_2(NO_3) \cdot (2 + j)\,TBP + NO_3^-. \qquad (2)$$
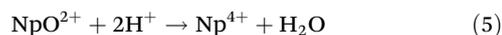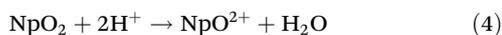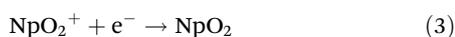
The coordination of an additional TBP ligand in the Np(v) complex is presumed based on the availability of two additional coordination sites from the departure of a bidentate nitrate. It is possible that water co-extracted into the organic phase occupies the final vacant coordination site. With the scheme proposed in eqn (2), the Np(v) complex is expected to be larger than the Np(vi) complex due to the additional TBP molecule coordinated to Np(v). The difference in calculated diffusion coefficients for each species supports this, with Np(v) and Np(vi) in TBP having values of $(3.5 \pm 0.6) \times 10^{-7}$ cm^2 s^{-1} and $(4.3 \pm 0.8) \times 10^{-7}$ cm^2 s^{-1}, respectively. In keeping with prior results reported for cerium[17] and plutonium[10] in neat TBP, these values are considerably smaller than the diffusion coefficient reported for Np(vi) in 3 M HNO$_3$, which is 2.31×10^{-6} cm^2 s^{-1}.[27] A combination of factors generate this difference, including the size of TBP ligands and the increased viscosity of undiluted TBP.[33] With the viscosity of the neat TBP–HNO$_3$ mixture under consideration being estimated at 5.15 mPa s, the Stokes–Einstein equation shows that most of the decrease in diffusion coefficient going from aqueous to organic media is due to the increased viscosity.[27,33]

When considering the entirety of the available solvent window for TBP–HNO$_3$ on a glassy carbon electrode, solutions containing bulk Np(vi) present intriguing redox activity. The behavior shown in Fig. 2 for neat TBP equilibrated with 4 M HNO$_3$ has been observed by Ikeda-Ohno et al. in both HClO$_4$ and HNO$_3$/NH$_4$NO$_3$ aqueous media.[34] They assigned the large, low-potential reduction event to be the Np(v) → Np(iii) reaction.

Fig. 7 (a) Differential pulse voltammograms demonstrating the effect of HDBP concentration on the position of the Np(vi/v) reduction potential in 50% TBP. Working electrode: 10 μm Pt ultramicroelectrode; counter electrode: Pt coil; reference electrode: Pt/PPy; [Np] = 0.95 mM. (b) Dependence of the DPV peak potential for the Np(vi/v) couple on the logarithm of HDBP concentration in 50% TBP. The line is the least-squares fit line and is described by $E_p = (-0.054 \pm 0.015)\log[\text{TBP}] + (0.48 \pm 0.04)$ with $R^2 = 0.915$.

Because the magnitude of peak current of the −0.494 V reduction event in Fig. 2 indicates a two-electron transfer, this is assigned as the organic-phase Np(v) → Np(iii) reduction. This is shifted negatively compared with Ikeda-Ohno's aqueous results, where the reduction peak appeared at approximately −0.31 V *vs.* Ag/AgCl in an aqueous 4.4 M HNO₃/6.0 M NH₄NO₃ solution.[34] Due to the high overpotential necessitated by the kinetic difficulty of breaking the neptunyl Np=O bonds, the reduction of Np(v) proceeds straight to Np(iii), as has also been observed in aqueous mineral acids.[24,35] The potential requirements for re-oxidation of Np(iii) to Np(iv) are much milder, however, and thus the −0.189 V feature in Fig. 2 is assigned as the Np(iii) → Np(iv) oxidation. The relatively small magnitude of this peak in TBP–HNO₃ is similar to observations in aqueous media,[34] and reinforces the conclusion from the Np(iv) CVs that the Np(iii) state is unstable in the TBP–HNO₃ solvent. Given the difficulty of observing oxidation of Np(iv) in TBP and in other systems,[35] it appears that there is no Np(iv) → Np(v) or Np(vi) oxidation event in the CV; rather, the oxidation peak at positive potentials is that of Np(v) → Np(vi). The relatively small 1 mm GCE does not consume all Np(v) and Np(vi) in solution on the reduction sweep; thus, there is residual Np(v) that is oxidized on the return sweep.

The wide-range DPV of a bulk Np(vi) solution in TBP presents much the same perspective as the CV, but the higher resolution of DPV also reveals a sharp peak at −0.31 V in the negative (reduction) sweep. While the exact identity of this sharp peak is not known, it is almost certainly related to the reduction of pentavalent neptunyl, NpO₂⁺. If transfer of the first electron in reduction of neptunyl (ligands omitted for clarity) is similar to that of pentavalent vanadyl ion, VO₂⁺, in aqueous media,[36] it may proceed as

$$NpO_2^+ + e^- \rightarrow NpO_2 \qquad (3)$$

$$NpO_2 + 2H^+ \rightarrow NpO^{2+} + H_2O \qquad (4)$$

$$NpO^{2+} + 2H^+ \rightarrow Np^{4+} + H_2O \qquad (5)$$

and this process may contribute to the DPV peak observed. Alternately, the sharpness of the peak may indicate that it is the complete two-electron reduction, Np(v) → Np(iii). In this case, Np(v) could be reduced to Np(iii), which given its instability could re-oxidize to Np(iv) as it diffuses near the electrode and produce Np(iv) for the broader reduction peak that follows at −0.39 V. Another explanation for the sharp peak would be a neptunium species deposited on the electrode that is reduced at −0.31 V; sharp peaks are typically associated with differential pulse stripping voltammetry.[37] This would align with the suspicion that adsorption-based processes are present in the Np–TBP system on glassy carbon, as has been observed with Pu–TBP.[10]

Attempts at wide-range CV and DPV scans of the bulk-Np(iv) system yield further insight into the kinetics of the Np(iii)/Np(iv)/Np(v)/Np(vi) system in neat TBP–HNO₃. Even with repeated scanning, no redox activity was observed in the Np(vi/v) potential region (SI Fig. S7). Thus, the kinetic barrier to re-forming neptunyl oxo bonds is greater than that hindering their breakage. In complexing aqueous media (*i.e.*, HNO₃ or H₂SO₄), Np⁴⁺ is so kinetically inert that that the potential required to oxidize it to NpO₂⁺ or NpO₂²⁺ lies beyond the potential at which water electrolysis occurs (GC electrode material).[35] The same appears to be the case here, where stabilization of Np(iv) through coordination by TBP and NO₃⁻, along with the kinetic barrier of re-forming Np=O bonds, prevents Np(v) formation.

While Bahri *et al.* found the Pu(iv/iii) redox reaction to have reversible electron transfer in neat TBP, the results of this work highlight contrasting behavior in the Np(iv/iii) couple.[10] Even on inert glassy carbon, reversible CV waves were not obtained in a bulk Np(iv) solution. This irreversible behavior is likely driven by the instability of Np(iii) in acid-laden TBP. The Np(iii) state is in general less stable than Pu(iii), with the aqueous (1 M HNO₃) redox potentials for the Np(iv/iii) and Pu(iv/iii) redox couples occurring at −0.07 (ref. 28) and 0.73 V *vs.* Ag/AgCl, respectively.[38] Overall, the negative shift of the Np(iv/iii) couple in TBP–HNO₃ shows a stabilization of Np(iv), which follows the pattern established by extracted Pu(iv).[10]

Additional appreciation for the stability of neptunium oxidation states in TBP may be gleaned from spectrophotometric investigation of organic-phase bulk electrolysis. Whereas true spectroelectrochemistry of the Np(vi/v) couple in 1 M HNO₃ has demonstrated complete reduction of Np(vi), in neat TBP equilibrated with 1 M HNO₃, large reducing overpotentials were not able to fully eliminate Np(vi).[28] Furthermore, the Np(v) absorption at 977 nm decreased by 82% in a 30-minute period after application of a −52 mV overpotential, underscoring the instability of Np(v) in TBP–HNO₃. Despite this, the spectral signatures for disproportionation–absorptions at 709 nm (ref. 31) for Np(iv) or at 1004 nm (ref. 30) for the Np(iv)–Np(v) cation–cation interaction – were not observed, suggesting that Np(v) is lost to oxidation in this system. While Sarsfield *et al.* observed increased Np(v) disproportionation in 30% TBP, they also noted that disproportionation increases as the solvent's dielectric constant decreases.[30] In the undiluted TBP–HNO₃ system, the absence of dodecane ($\varepsilon = 8.34$) and the increased water ($\varepsilon = 80.2$) and nitric acid ($\varepsilon = 19.0$) concentrations from extraction by TBP will contribute to a higher dielectric constant and thus hinder disproportionation.[39]

From a vis-NIR spectrum taken of the Np(vi)–TBP solution immediately after extraction, the molar absorptivity for Np(vi) in neat TBP at 569 nm is calculated to be $12.9 \pm 1.6 \text{ M}^{-1} \text{ cm}^{-1}$, which is approximately twice the intensity observed in 30% TBP.[30] Prior to beginning bulk electrolysis, a miniscule absorption for Np(v) was recorded in the solution. This is a predictable result based on the open-circuit potential of the TBP–HNO₃. Based on the Nernst equation, the 0.89 V open-circuit potential of the metal-free TBP (1 M HNO₃) solution should contain 0.38% Np(v) at rest, considering that the Np(vi/v) redox potential in this solution is 0.747 V. By extrapolation of data from Marchenko *et al.*, the molar absorptivity at 977 nm for Np(v) in the TBP–HNO₃ solution may be estimated at 229.5 $\text{M}^{-1} \text{ cm}^{-1}$.[31] From this a Np(v) absorption intensity of 0.0033
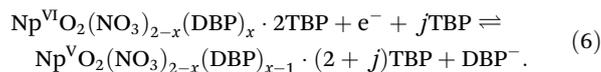
is calculated, which agrees well with the observed value of 0.0029. The Np(v) absorption at 1086 nm has not been reported previously for TBP solutions, but it is likely a blue-shift of the 1092 nm band previously-reported in aqueous nitric acid.[27,28] Besides the main absorption at 569 nm, other Np(vi) bands that are more clearly distinguishable in TBP than in aqueous media include 520, 544.5, 605, and 633 nm.

For the Np(vi/v) couple in TBP diluted to various levels with dodecane, distortion of the DPV response is observed, especially with 60% or more dodecane (40% or less TBP). This is due to a dramatic decrease in solvent conductivity, due in part to a change in nitric acid speciation from dissociated to associated as dilution increases.[8] Two experimental choices that enable useable data collection at such dilution levels are important to highlight. First, the demonstration of TBA OTf as a suitable electrolyte in this system represents an improvement over previous investigations of metal redox in TBP solvents, where tetra-*n*-butylammonium tetrafluoroborate proved unstable in TBP–HNO$_3$.[10] In PUREX-type TBP/dodecane mixtures, neither the tetrafluoroborate nor hexafluorophosphate salts of tetrabutylammonium are soluble to an appreciable degree. Second, this report demonstrates that Pt can be a suitable working electrode material in TBP–HNO$_3$ media, in contrast to previous indications that only glassy carbon functioned in this solvent.[8] It is hypothesized that previous reports of Pt unsuitability in TBP–HNO$_3$ were confounded by electrode passivation due to cerium, which was the analyte in question. Using noble metal electrode materials in this system is crucial, as it enables the use of ultramicroelectrodes, which with their 10 μm diameter (and coupled with rigorous Faraday cage noise suppression) allow accurate measurement of the $\sim 10^{-11}$ A currents attainable in highly diluted TBP–dodecane systems.

As the DPV peak potential for the Np(vi/v) couple is followed through dilution of TBP from 100% to 30%, a shift of 101 ± 26 mV per decade is observed (Fig. 6). The Np(v) state likely becomes less stable as the solvent's dielectric constant decreases,[30] which would be observed as the negative shift in potential with dilution. This shift is intermediate of that expected from a one-ligand or a two-ligand exchange accompanying by a one-electron reduction (59 mV per decade and 118 mV per decade, respectively), suggesting that j, the average number of additional TBP ligands binding on reduction of Np(vi), is between one and two (eqn (2)). Little is known regarding the organic-phase speciation of Np(v) due to its nearly-unextractable nature.[2] That said, with the larger neptunium radius in the NpO$_2^+$ moiety[40] and the two coordination sites left by the departing nitrate, addition of at least one TBP seems plausible, especially given the amount of TBP available in >30% solutions.

The systematic decrease in Np(vi/v) DPV peak potential on addition of HDBP in 50% TBP also has clear implications for separations of used nuclear fuel where radiolysis is a concern. For the first time, direct electrochemical evidence is presented for HDBP-induced stabilization of an actinide's hexavalent state in the VI/V couple. In the Np(vi/v) system presented here, the peak potential shifts by −54 ± 15 mV per decade with

respect to HDBP concentration, indicating a loss of one DBP$^-$ ligand upon reduction:

$$\begin{aligned} Np^{VI}O_2(NO_3)_{2-x}(DBP)_x \cdot 2TBP + e^- + jTBP \rightleftharpoons \\ Np^VO_2(NO_3)_{2-x}(DBP)_{x-1} \cdot (2+j)TBP + DBP^-. \end{aligned} \quad (6)$$

The loss of one DBP$^-$ anion upon reduction aligns with previous solvent extraction slope analysis studies in 30% TBP, which were consistent with a 1 : 2 Np : HDBP ratio for Np(vi) and a 1 : 1 ratio for Np(v) at low acidities.[18]

Additionally, the electrochemical stabilization of Np(vi) by HDBP provides direct explanation for the inhibition of reductive stripping previously observed in irradiated or HDBP-containing solvents.[18] In a reductive strip step, a metal-loaded organic phase is contacted with an aqueous phase containing a reducing agent to reduce the metal ions of interest from a well-extracted oxidation state to a poorly-extracted one, causing stripping. The nitrous acid used as a reducing agent in the previous study was insufficient to overcome the stabilization of Np(vi) in the degraded solvent.[18] The current work indicates that in adding 8 mM HDBP (the concentration expected after ~80 kGy gamma dose[32]) to previously-clean 50% TBP, the Np(vi/v) couple shifted by −91 mV, illustrating the need for stronger reductants (or aqueous complexants) to overcome the effect of radiolytic HDBP in neptunium reductive strip procedures.

Beyond only providing insight into the behavior of neptunium in neat and diluted TBP–HNO$_3$ systems, these results shed broader light on actinide behavior in reprocessing plant solvents. For the Np(vi/v), Pu(vi/v), and Am(vi/v) couples, a trend emerges that negative shifts in reduction potential between aqueous and TBP solvents grow moving across the actinide series. Shifts in potential from (aqueous → organic) measured thus far are Np(vi/v), −158 mV; Pu(vi/v), −188 mV;[10] and Am(vi/v), −770 mV.[9] This reflects the increasing instability of the An(v) state as much as it does the stabilization of An(vi) due to TBP complexation. The findings presented in this work also inform predictions for plutonium behavior in PUREX-type reprocessing systems. Extending the results of the TBP dilution study, it is plausible to expect that the Pu(iv/iii) redox potential also will decrease from the reported value of 0.554 V *vs.* Ag/AgCl when changing from neat TBP to diluted TBP. Additionally, by combining the present neptunium results with previous studies using Ce(iv),[8,17] it is possible to predict that the presence of radiolytic HDBP will electrochemically stabilize Pu(iv), thus hindering the reductive stripping step of the PUREX process.

Conclusion

Investigation of the electrochemistry of neptunium in both neat and diluted TBP creates a complementary picture of its overall behavior in reprocessing-relevant organic solvents. Using undiluted, acid-equilibrated TBP as an electrochemical solvent allowed broad investigation of neptunium's redox

couples and showed that voltammetry starting from neptunyl species in TBP largely resembles that of aqueous neptunium, with a quasireversible Np(VI/V) couple as well as direct Np(V) → Np(III) reduction. The positions of both the Np(VI/V) and Np(IV/III) couples are shifted to lower potentials in TBP *versus* their aqueous counterparts, however, revealing substantial stabilization of both Np(IV) and Np(VI) through complexation with TBP. Conversely, the poorly extracted Np(III) and Np(V) species are demonstrated to be less stable in TBP than in aqueous media through voltammetric and spectrophotometric means.

Although the electrochemical properties of diluted TBP are more difficult, being able to use diluted TBP as a solvent for electrochemical studies removes approximations from understanding neptunium's behavior in real-world systems. Lowering the TBP concentration by dilution causes a negative shift in the Np(VI/V) couple, which likely indicates a further destabilization of the Np(V) state. With experimental innovations, electrochemical measurements of an actinide in the 30% TBP PUREX process solvent are demonstrated for the first time, showing the shift in redox potential and highlighting the approximation made by making electrochemical measurements in undiluted TBP. In 50% TBP, HDBP causes a further negative shift in the Np(VI/V) couple potential, indicating that complexation by dibutylphosphate hinders the reduction of Np(VI) in the organic phase.

The experimental methodologies proven in this work have broad applicability beyond only neptunium–TBP electrochemistry. Miniaturization of the working electrode in tandem with exploration of supporting electrolytes enables electrochemistry in far more dilute TBP solvents than previously reported. While observations on the neptunium system have predictive power for plutonium in similar solutions (*e.g.* Pu(IV) will be stabilized by HDBP against reductive stripping), measurements of plutonium in 30% TBP will yield the highest accuracy data. The techniques demonstrated in this work will also be useful for measurements in other diluents, such as the industrial choice of odorless kerosene. Beyond just the Pu(IV/III) and Np(VI/V) couples relevant to the standard PUREX process, we believe that the methods demonstrated herein have applicability to investigation of other separations such as that of americium and curium. The SESAME (Selective Extraction and Separation of Americium by Means of Electrolysis) process proposes extraction of highly-oxidized Am(VI) by TBP but has not been successfully implemented due to uncertainty in maintaining the Am(VI) state.[41] Investigation of the organic-phase redox couples of americium may bring this idea nearer to success. Outside the field of nuclear separations, redox-based solvent extraction separations have been proposed for critical mineral recovery using the semi-accessible Tb(IV/III) and Pr(IV/III) couples,[42] and successful processes have been tested manipulating the Eu(III/II) couple.[43] Organic-phase metal redox chemistry is also a key component of certain vanadium/molybdenum separations[43] and in methods of iron removal during gallium/indium extraction from zinc ores.[44]

Conflicts of interest

The authors declare no conflicts of interest.

Data availability

The data supporting this article have been included as part of the supplementary information (SI). Supplementary information: comparison of DPV data before and after smoothing, DPV and CV plots for Np(IV) and Np(VI), the background CV for glassy carbon in TBP–HNO$_3$, the DPV response of HNO$_2$ in TBP–HNO$_3$, an additional visible-NIR spectrum for Np(VI/V) bulk electrolysis, conductivities of TBP–dodecane mixtures, and additional voltammograms for the ultramicroelectrode response of the Np(VI/V) couple in undiluted and 30% TBP. The "W" cell setup is also depicted and the Nernst relationship between [HDBP] and the measured reduction is derived. See DOI: https://doi.org/10.1039/d5dt01823d.

Acknowledgements

References

1   J. P. Glatz, P. Souček and R. Malmbeck, Key Challenges in Advanced Reprocessing of Spent Nuclear Fuels, in *Reprocessing and Recycling of Spent Nuclear Fuel*, 2015, pp. 49–62. DOI: 10.1016/B978-1-78242-212-9.00003-4.

2   R. S. Herbst, P. Baron and M. Nilsson, Standard and Advanced Separation: PUREX Processes for Nuclear Fuel Reprocessing, in *Advanced Separation Techniques for Nuclear*

Fuel Reprocessing and Radioactive Waste Treatment, Woodhead Publishing, 2011, pp. 141–175.

3 G. J. Lumetta, J. R. Allred, S. A. Bryan, G. B. Hall, T. G. Levitskaia, A. M. Lines and S. I. Sinkov, Simulant Testing of a Co-Decontamination (CoDCon) Flowsheet for a Product with a Controlled Uranium-to-Plutonium Ratio, *Sep. Sci. Technol.*, 2019, **54**(12), 1977–1984, DOI: 10.1080/01496395.2019.1594899.

4 E. Aneheim, C. Ekberg, A. Fermvik and M. R. S. Foreman, Development of a Novel GANEX Process, in *Nuclear Energy and the Environment; ACS Symposium Series*, American Chemical Society, 2010, vol. 1046, pp. 119–130. DOI: 10.1021/bk-2010-1046.ch010.

5 P. Baron, S. M. Cornet, E. D. Collins, G. DeAngelis, G. Del Cul, Y. Fedorov, J. P. Glatz, V. Ignatiev, T. Inoue, A. Khaperskaya, I. T. Kim, M. Kormilitsyn, T. Koyama, J. D. Law, H. S. Lee, K. Minato, Y. Morita, J. Uhlíř, D. Warin and R. J. Taylor, A Review of Separation Processes Proposed for Advanced Fuel Cycles Based on Technology Readiness Level Assessments, *Prog. Nucl. Energy*, 2019, **117**, 103091, DOI: 10.1016/j.pnucene.2019.103091.

6 V. I. Marchenko, V. S. Koltunov and K. N. Dvoeglazov, Kinetics and Mechanisms of Redox Reactions of U, Pu, and Np in Tributyl Phosphate Solutions, *Radiochemistry*, 2010, **52**(2), 111–126, DOI: 10.1134/S1066362210020013.

7 V. I. Marchenko, V. N. Alekseenko and K. N. Dvoeglazov, Organic Reductants of Pu and Np Ions in Wet Technology for Spent Nuclear Fuel Reprocessing, *Radiochemistry*, 2015, **57**(4), 366–377, DOI: 10.1134/S1066362215040050.

8 M. A. Bahri, A. Ruas, P. Moisy and E. Labbé, Electrochemical Behavior of Cerium(IV) Species in *n*-Tributylphosphate, *Electrochim. Acta*, 2015, **169**, 1–6, DOI: 10.1016/j.electacta.2015.04.014.

9 H. Mokhtari and S. Picart, Measurement of Some Actinides Redox Potentials in TBP Medium with Ultramicroelectrode, *Recent Adv. Actin. Sci.*, 2006, 632–634.

10 M. A. Bahri, A. Ruas, E. Labbé and P. Moisy, Electrochemical Characterization of Plutonium in *n*-Tributyl Phosphate, *Dalton Trans.*, 2017, **46**(15), 4943–4949, DOI: 10.1039/C6DT04765C.

11 P. K. Verma, B. Mahanty, R. B. Gujar and P. K. Mohapatra, Neptunium – Tri-*n*-Butyl Phosphate Complexes in Room Temperature Ionic Liquids: Extraction and Spectroelectrochemical Studies, *J. Mol. Liq.*, 2021, **325**, 115144, DOI: 10.1016/j.molliq.2020.115144.

12 B. J. Mincher, M. Precek, S. P. Mezyk, G. Elias, L. R. Martin and A. Paulenova, The Redox Chemistry of Neptunium in γ-Irradiated Aqueous Nitric Acid, *Radiochim. Acta*, 2013, **101**(4), 259–265, DOI: 10.1524/ract.2013.2013.

13 Y. Ban, Y. Hakamatsuka, N. Tsutsui, S. Urabe, H. Hagiya and T. Matsumura, Spectroscopic Study of Np(V) Oxidation to Np(VI) in 3 mol/dm^3 Nitric Acid at Elevated Temperatures, *Radiochim. Acta*, 2014, **102**(9), 775–780, DOI: 10.1515/ract-2013-2193.

14 B. J. Mincher, M. Precek, S. P. Mezyk, L. R. Martin and A. Paulenova, The Role of Oxidizing Radicals in Neptunium Speciation in γ-Irradiated Nitric Acid, *J. Radioanal. Nucl. Chem.*, 2013, **296**(1), 27–30, DOI: 10.1007/s10967-012-1937-1.

15 A. Tahraoui and J. H. Morris, Decomposition of Solvent Extraction Media during Nuclear Reprocessing: Literature Review, *Sep. Sci. Technol.*, 1995, **30**(13), 2603–2630.

16 B. J. Mincher, S. P. Mezyk and L. R. Martin, A Pulse Radiolysis Investigation of the Reactions of Tributyl Phosphate with the Radical Products of Aqueous Nitric Acid Irradiation, *J. Phys. Chem. A*, 2008, **112**(28), 6275–6280, DOI: 10.1021/jp802169v.

17 J. R. Dunbar and M. P. Jensen, Influence of Di-*n*-Butyl Phosphoric Acid on Cerium Redox and Speciation in Tri-*n*-Butyl Phosphate, *Inorg. Chem.*, 2024, **63**(28), 12839–12848, DOI: 10.1021/acs.inorgchem.4c01309.

18 J. R. Dunbar, D. R. Peterman and M. P. Jensen, Radiolytic Alterations to Neptunium Extraction and Redox in 30% Tri-*n*-Butyl Phosphate, *Radiochim. Acta*, 2025, **113**(5), 361–372, DOI: 10.1515/ract-2024-0354.

19 P. K. Verma and P. K. Mohapatra, Fate of Neptunium in Nuclear Fuel Cycle Streams: State-of-the Art on Separation Strategies, *Radiochim. Acta*, 2022, **110**(6–9), 527–548, DOI: 10.1515/ract-2022-0008.

20 J. Ghilane, P. Hapiot and A. J. Bard, Metal/Polypyrrole Quasi-Reference Electrode for Voltammetry in Nonaqueous and Aqueous Solutions, *Anal. Chem.*, 2006, **78**(19), 6868–6872, DOI: 10.1021/ac060818o.

21 H. Yoshida, Solvent Extraction Studies of Thiocyanate Complex of the Lanthanides, *J. Inorg. Nucl. Chem.*, 1962, **24**, 1257–1265.

22 G. A. Burney and R. M. Harbour, *Radiochemistry of Neptunium*, The National Academies Press, Washington, DC, 1974, DOI: 10.17226/20072.

23 M. R. Antonio, T. J. Demars, M. Audras and R. J. Ellis, Third Phase Inversion, Red Oil Formation, and Multinuclear Speciation of Tetravalent Cerium in the Tri-*n*-Butyl Phosphate–*n*-Dodecane Solvent Extraction System, *Sep. Sci. Technol.*, 2018, **53**(12), 1834–1847, DOI: 10.1080/01496395.2017.1281303.

24 Y. Kitatsuji, T. Kimura and S. Kihara, Reduction Behavior of Neptunium(V) at a Gold or Platinum Electrode during Controlled Potential Electrolysis and Procedures for Electrochemical Preparations of Neptunium(IV) and (III), *J. Electroanal. Chem.*, 2010, **641**(1–2), 83–89, DOI: 10.1016/j.jelechem.2009.12.015.

25 W. Davis, J. Mrochek and C. J. Hardy, The System: Tri-n-Butyl Phosphate (TBP)-Nitric Acid-Water—I Activities of TBP in Equilibrium with Aqueous Nitric Acid and Partial Molar Volumes of the Three Components in the TBP Phase, *J. Inorg. Nucl. Chem.*, 1966, 2001–2014.

26 V. S. Koltunov, R. J. Taylor, V. I. Marchenko, E. H. A. Mezhov, G. I. Zhuravleva, K. N. Dvoeglazov and O. A. Savilova, Kinetics and Mechanisms of Np(VI) and Np(V) Reductions by U(IV) in TBP Solutions, *J. Nucl. Sci. Technol.*, 2002, **39**, 351–354, DOI: 10.1080/00223131.2002.10875481.

27 S.-Y. Kim, T. Asakura, Y. Morita, G. Uchiyama and Y. Ikeda, Electrochemical and Spectroelectrochemical Properties of Neptunium(vi) Ions in Nitric Acid Solution, *J. Radioanal. Nucl. Chem.*, 2004, **262**(2), 311–315.

28 S. Chatterjee, S. A. Bryan, A. J. Casella, J. M. Peterson and T. G. Levitskaia, Mechanisms of Neptunium Redox Reactions in Nitric Acid Solutions, *Inorg. Chem. Front.*, 2017, **4**(4), 581–594, DOI: 10.1039/c6qi00550k.

29 A. Bard and L. Faulkner, in *Electrochemical Methods*, Wiley, New York, 2nd edn, 2001.

30 M. J. Sarsfield, R. J. Taylor and C. J. Maher, Neptunium(v) Disproportionation and Cation-Cation Interactions in TBP/Kerosene Solvent, *Radiochim. Acta*, 2007, **95**(12), 677–682, DOI: 10.1524/ract.2007.95.12.677.

31 V. I. Marchenko, V. S. Koltunov, O. A. Savilova and G. I. Zhuravleva, Redox Kinetics of U, Pu, and Np in TBP Solutions: VI. Reactions of Neptunium and Plutonium with Organic Reducing Agents: Determination of the Final Oxidation States and Reaction Rates, *Radiochemistry*, 2001, **43**(3), 276–283.

32 D. R. Peterman, B. J. Mincher, C. L. Riddle and R. D. Tillotson, *Summary Report on Gamma Radiolysis of TBP/n-Dodecane in the Presence of Nitric Acid Using the Radiolysis/Hydrolysis Test Loop*; INL/EXT-10-19866; Idaho National Lab. (INL), Idaho Falls, ID (United States), 2010. DOI: 10.2172/993164.

33 D. G. Tuck, Solvent Extraction Studies. Part 4.—Viscosity Measurements on the System Nitric Acid + tri-*n*-Butyl Phosphate, *Trans. Faraday Soc.*, 1961, **57**(0), 1297–1304, DOI: 10.1039/TF9615701297.

34 A. Ikeda-Ohno, C. Hennig, A. Rossberg, H. Funke, A. C. Scheinost, G. Bernhard and T. Yaita, Electrochemical and Complexation Behavior of Neptunium in Aqueous Perchlorate and Nitrate Solutions, *Inorg. Chem.*, 2008, **47**(18), 8294–8305, DOI: 10.1021/ic8009095.

35 H. Aoyagi, Y. Kitatsuji, Z. Yoshida and S. Kihara, Rapid and Quantitative Electrolytic Preparation and Speciation of Neptunium Ions of Various Oxidation States Using Multi-Step Column Electrodes, *Anal. Chim. Acta*, 2005, **538**(1–2), 283–289, DOI: 10.1016/j.aca.2005.02.035.

36 J. Lee, J. T. Muya, H. Chung and J. Chang, Unraveling V(v)-V(iv)-V(iii)-V(ii) Redox Electrochemistry in Highly Concentrated Mixed Acidic Media for a Vanadium Redox Flow Battery: Origin of the Parasitic Hydrogen Evolution Reaction, *ACS Appl. Mater. Interfaces*, 2019, **11**(45), 42066–42077, DOI: 10.1021/acsami.9b12676.

37 M. M. Ghoneim, A. M. Hassanein, E. Hammam and A. M. Beltagi, Simultaneous Determination of Cd, Pb, Cu, Sb, Bi, Se, Zn, Mn, Ni, Co and Fe in Water Samples by Differential Pulse Stripping Voltammetry at a Hanging Mercury Drop Electrode, *Fresenius' J. Anal. Chem.*, 2000, **367**(4), 378–383, DOI: 10.1007/s002160000410.

38 A. Fallet, N. Larabi-Gruet, S. Jakab-Costenoble and P. Moisy, Electrochemical Behavior of Plutonium in Nitric Acid Media, *J. Radioanal. Nucl. Chem.*, 2016, **308**(2), 587–598, DOI: 10.1007/s10967-015-4423-8.

39 *CRC Handbook of Chemistry and Physics*, ed. W. M. Haynes, CRC Press, Boca Raton, Florida, 95th edn, 2014.

40 E. Mauerhofer, K. P. Zhernosekov and F. Rösch, Limiting Transport Properties and Hydration Numbers of Actinyl Ions in Pure Water, *Radiochim. Acta*, 2004, **92**(1), 5–10, DOI: 10.1524/ract.92.1.5.25405.

41 W. H. Runde and B. J. Mincher, Higher Oxidation States of Americium: Preparation, Characterization and Use for Separations, *Chem. Rev.*, 2011, **111**(9), 5723–5741, DOI: 10.1021/cr100181f.

42 N. T. Rice, I. A. Popov, D. R. Russo, J. Bacsa, E. R. Batista, P. Yang, J. Telser and H. S. La Pierre, Design, Isolation, and Spectroscopic Analysis of a Tetravalent Terbium Complex, *J. Am. Chem. Soc.*, 2019, **141**(33), 13222–13233, DOI: 10.1021/jacs.9b06622.

43 T. Hirai and I. Komasawa, Separation of Rare Metals by Solvent Extraction Employing Reductive Stripping Technique, *Miner. Process. Extr. Metall. Rev.*, 1997, **17**(1–4), 81–107, DOI: 10.1080/08827509708914143.

44 S. Nishihama, T. Hirai and I. Komasawa, Mechanism of Photoreductive Stripping of Iron(iii) in a Liquid–Liquid Extraction System and Its Application for a Hydrometallurgical Process, *Ind. Eng. Chem. Res.*, 1999, **38**(12), 4850–4856, DOI: 10.1021/ie990345u.